Title

Identification of Lineage-Specific Transcription Factors That Prevent Activation of Hepatic Stellate Cells and Promote Fibrosis Resolution

Journal

Gastroenterology, 158(6)

ISSN

0016-5085

Authors

Liu, Xiao
Xu, Jun
Rosenthal, Sara
et al.

Publication Date

2020-05-01

DOI

10.1053/j.gastro.2020.01.027

Peer reviewed

HHS Public Access

Author manuscript

Gastroenterology. Author manuscript; available in PMC 2021 May 01.

Published in final edited form as:

Gastroenterology. 2020 May ; 158(6): 1728–1744.e14. doi:10.1053/j.gastro.2020.01.027.

Identification of Lineage-specific Transcription Factors That Prevent Activation of Hepatic Stellate Cells and Promote Fibrosis Resolution

Xiao Liu[1,2], **Jun Xu**[1,2], **Sara Rosenthal**[1,3], **Ling-juan Zhang**[4,5], **Ryan McCubbin**[1], **Nairika Meshgin**[1], **Linshan Shang**[2], **Yukinori Koyama**[1,2], **Hsiao-Yen Ma**[1], **Sonia Sharma**[6], **Sven Heinz**[1], **Chris K. Glass**[7], **Chris Benner**[1], **David A. Brenner**[1], **Tatiana Kisseleva**[2,*]

[1]Dept.of Medicine, UCSD, La Jolla, California, USA

[2]Dept.of Surgery, UCSD, La Jolla, California, USA

[3]Dept.of Center for Computational Biology & Bioinformatics, UCSD, La Jolla, California, USA

[4]Department of Dermatology, UCSD, La Jolla, California, USA

[5]School of Pharmaceutical Sciences, Xiamen University, Xiamen, China

[6]La Jolla Institute for Immunology, La Jolla, California, USA

[7]Department of Cellular & Molecular Medicine, UCSD, La Jolla, California, USA

Abstract

Background & Aims—Development of liver fibrosis is associated with activation of quiescent hepatic stellate cells (qHSCs) into collagen type I-producing myofibroblasts (activated or aHSCs). Cessation of liver injury often results in fibrosis resolution and inactivation of aHSCs/ myofibroblasts into a quiescent-like state (iHSCs). We aimed identify molecular features of phenotypes of HSCs from mice and humans.

Methods—We performed studies with *Lrat*^{Cre}, *Ets1*-floxed, *Nf1*-floxed, *Ppar*γ-floxed, *Gata6*-floxed, *Rag2*$^{-/-}$γc$^{-/-}$, and C57/Bl6 (control) mice. Some mice were given carbon tetrachloride to induce liver fibrosis, with or without a PPARγ agonist. Livers from mice were analyzed by immunohistochemistry. qHSCs, aHSCs, and iHSCs were isolated from livers of *Col1*α*1*^{YFP} mice and analyzed by chromatin immunoprecipitation and sequencing. Human HSCs were isolated from livers denied for transplantation. We compared changes in gene expression patterns and epigenetic modifications (H3K4me2 and H3K27ac) in primary mouse and human HSCs. Transcription factors were knocked down with small hairpin RNAs in mouse HSCs.

[*]**Corresponding author:** Tatiana Kisseleva (tkisseleva@ucsd.edu).

Author contribution: XL – designed the study, collected data, wrote MS; JX – conducted PPARγ-related studies in mice, CB, SH – provided help with ChIP-Seq experimental design, data collection and analysis, wrote MS, SR, LZ, RM, NM, LS, YK, H-SM – provided help with data analysis; SS, CKG, DAB – provided support, critically reviewed the MS; TK – provided support, designed the study, wrote MS.

Conflict of interests: nothing to declare

Results—Motif enrichment identified ETS1, ETS2, GATA4, GATA6, IRF1, and IRF2 transcription factors as regulators of the mouse and human HSC lineage. Small hairpin RNA-knockdown of these transcription factors resulted in increased expression of genes that promote fibrogenesis and inflammation, and loss of HSC phenotype. Disruption of *Gata6* or *Ets1*, or *Nf1*or *Pparγ* (which are regulated by ETS1), increased the severity of carbon tetrachloride (CCl_4)-induced liver fibrosis in mice compared to control mice. Only mice with disruption of *Gata6* or *Pparg* had defects in fibrosis resolution after CCl_4 administration was stopped, associated with persistent activation of HSCs. Administration of a PPARγ agonist accelerated regression of liver fibrosis following CCl_4 administration in control mice but not in mice with disruption of *Pparγ*.

Conclusions—Phenotypes of HSCs from humans and mice are regulated by transcription factors including ETS1, ETS2, GATA4, GATA6, IRF1, and IRF2. Activated mouse and human HSCs can revert to a quiescent-like, inactivated phenotype. We found GATA6 and PPARγ to be required for inactivation of human HSCs and regression of liver fibrosis in mice.

Lay Summary

This study identified proteins that regulate genes that control activation of liver cells involved in development or resolution of fibrosis. These proteins might be targeted for treatment of liver fibrosis.

Graphical Abstract

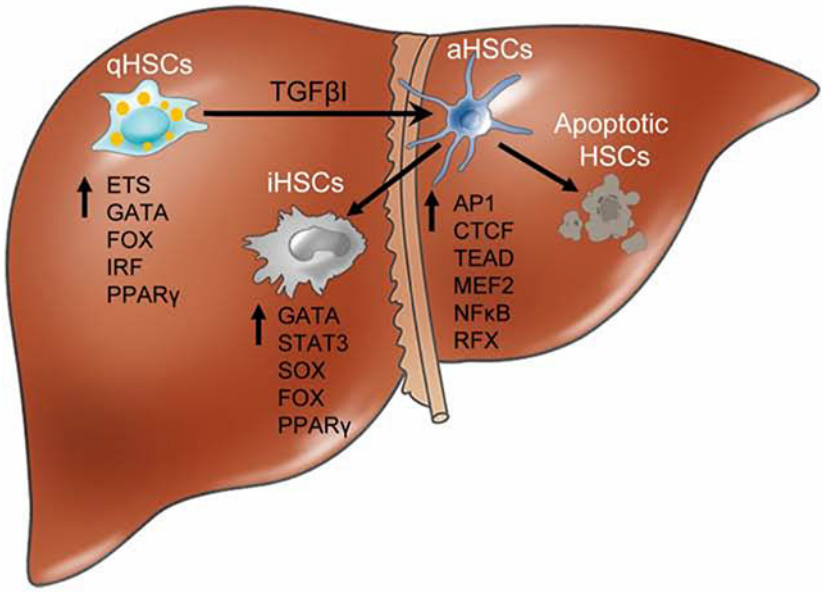

Transcriptional regulation of HSC phenotypes during development and regression of liver fibrosis. Under physiological conditions, HSCs exhibit a quiescent phenotype (qHSCs), which is associated with expression of ETS, GATA, FOX, IRF, PPARγ, and other transcription factors. In response to chronic injury and TGFβl, qHSCs upregulate AP-l, MET2, CTCF, TEAD, NFκB, RFX, and undergo activation into aHSCs/myofibroblasts. Upon cessation of fibrogenic stimuli, about half of aHSCs apoptose, while another half escape apoptosis, and inactivate (iHSCs). Inactivation of aHSCs is accompanied by re-expression of GATA6, PPARγ, SOX, FOX, STAT transcription factors. Regulation of HSC phenotypes is regulated on epigenetic level.

Keywords

resolution of liver fibrosis; inactivation of fibrogenic myofibroblasts; epigenetic regulation; lineage-determining transcription factors

Introduction

Chronic liver injury, such as alcoholic (ASH) and non-alcoholic (NASH) steatohepatitis, often results in liver fibrosis. Activated hepatic stellate cells (aHSCs) are the major source of Collagen Type I-producing myofibroblasts in fibrotic liver. Under physiological conditions, quiescent (q)HSCs store Vitamin A and express neural/adipogenic markers (GFAP, PPARγ, Adfp, Adipor1), but in response to injury rapidly upregulate fibrogenic genes and cytokines (Col1α1, α-SMA, TIMP1, IL-6)[1] and become aHSCs/myofibroblasts to produce the fibrous scar. Clinical and experimental studies have demonstrated that removal of the etiological stimuli of liver injury results in regression of liver fibrosis, and disappearance of aHSCs/myofibroblasts either by apoptosis (≈50%) or inactivation into a quiescent-like state (iHSCs, ≈50%)[1–3]. iHSCs gradually downregulate expression of fibrogenic genes, re-express some quiescence-associated genes (such as PPARγ), and express some unique genes.

The fate of human aHSCs/myofibroblasts during fibrosis resolution has not been determined. Here we demonstrate for the first time that, similar to murine HSCs, human aHSCs can inactivate when transplanted into an *in vivo* physiological environment that does not provide fibrogenic stimuli (such as livers of untreated $Rag2^{-/-}\gamma c^{-/-}$ mice). Inactivation of human HSCs resulted in downregulation of Col1α1, α-SMA, and re-expression of PPARγ, suggesting that human HSCs possess a remarkable plasticity, which makes them an attractive target for antifibrotic therapy.

HSC phenotypic states are regulated by the epigenome, which determines the accessibility of the regulatory elements of key response genes that are actively transcribed [4], establishes the cellular fate/lineage-specific identity, and delineates cellular responses under physiological conditions or in response to injury or stress[5]. We performed chromatin immunoprecipitation linked to massively parallel deep sequencing (ChIP-Seq) analysis and identified the sequence motifs enriched at promoters and enhancers marked by histone H3 lysine 4 dimethylation (H3K4me2)[5] and histone H3 lysine 27 acetylation (H3K27ac)[4] in mouse and human HSCs.

We identified ETS1/2, GATA4/6, and IRF1/2 as HSC lineage-specific TFs in mouse and human HSCs. *In vitro* shRNA-knockdown of these TFs resulted in the upregulation of fibrogenic and inflammatory genes in targeted HSCs, which lost their HSC lineage-specific phenotype. Development of this aberrant phenotype was mostly attributed to shRNA-knockdown of ETS1/2 and GATA4/6 (but not IRF1/2). In support, deletion of GATA4 in mesenchymal cells aggravated development of liver fibrosis in $G2^{GATA4-/-}$ mice[6]. We now demonstrate that $Lrat^{\Delta GATA6}$ mice (devoid of GATA6 in HSCs) are highly susceptible to CCl_4-induced injury (vs wt littermates). Since tissue-specific ablation of ETS1/2 was often associated with embryonic lethal phenotype[7], to gain the insight into the role of ETS1 in HSC biology, the ETS1 target genes NF1 and PPARγ were evaluated. CCl_4-induced liver

fibrosis was exacerbated in both Lrat$^{\Delta NF1}$ and Lrat$^{\Delta PPAR\gamma}$ mice. Inactivation of HSCs was associated with re-expression of PPARγ (but not NF1). In support, a marked delay in fibrosis resolution was observed only in Lrat$^{\Delta PPAR\gamma}$ mice, due to a failure of PPARγ-deficient HSCs to inactivate, implicating PPARγ (but not NF1) in the pathogenesis of HSC inactivation. Therapeutic administration of the PPARγ agonist rosiglitasone accelerated regression of CCl_4 liver fibrosis in wt mice (but not in Lrat$^{\Delta PPAR\gamma}$ mice), and effectively suppressed activation of human HSCs, underlining the critical role of PPARγ signaling in HSCs for regression of liver fibrosis.

Materials and Methods

Mice

Collagen1α1^{Cre} mice[1], Lrat^{Cre} mice (gift of Dr. Schwabe[8]), ETS1-floxed mice (gift of Dr. Kee[9]), NF1-floxed mice (gift of Dr. Parada[10]), PPARγ-floxed mice (#2651605), Rosa26flox-stop-flox-YFP mice (#006148), Gata6-floxed mice (#008196), and Rag2$^{-/-}\gamma$c$^{-/-}$ mice (#014593, Jackson Labs) were maintained under specific pathogen-free conditions at UCSD (protocol S07088 approved by IACUC).

Experimental model of liver fibrosis regression, isolation of mouse HSCs

Col1α1^{YFP} mice generated by crossing Col1α1^{Cre} x Rosa26$^{f/f\text{-}YFP}$ mice) were left uninjured (n=8), subjected to CCl_4 (1:4 in corn oil, 200µl, 12 ×, oral gavage, n=6), followed by regression of liver fibrosis (10 days, n=10, and 1 month, n=12). Freshly isolated qHSCs, aHSCs, and iHSCs (10 d, 1 mo) were isolated from livers of these mice using pronase/collagenase methods[1], sort purified for Vitamin A^{+}±YFP^{+} cells, and analyzed by the Whole Mouse Genome Microarray (1×10^6 cells/condition), or ChIP-Seq.

Chromatin immunoprecipitation (ChIP) and sequencing

mHSCs or hHSCs ($\approx 3 \times 10^6$ cells/condition) were cross-linked [5], chromatin was sheared (250–350 bp), and subjected to immunoprecipitation with H3K4me2 (2 µg, Millipore 07–030) or H3K27ac (2 µg, Active Motif 39133) or IgG. The protein-DNA crosslinks were reversed, the DNA fragments were used to generate sequencing library, and subjected to deep sequencing (Illumina HiSeq 2000). ChIP-seq reads were aligned to the human (hg38) or mouse (mm10) genomes using bowtie2[11]. ChIP-seq analysis was performed using HOMER [5] of uniquely alignable reads (MAPQ >=5). See supplemental materials for details.

Immunohistochemistry

Formalin-fixed mouse livers were stained with Sirius Red and anti-F4/80 (eBioscience, 14–4801-82 1:200), anti-αSMA (Abcam, ab5694 1:200), and anti-desmin (Abcam15200 1:100) Abs, followed by HRP conjugated secondary Ab (Vector Laboratories, MP-7401; MP-7444).

Immunocytochemistry

Primary human HSCs were first fixed by paraformaldehyde than stained with anti-desmin (Ab15200 1; 100), anti-GFAP (Abcam7260 1:100), and anti-TE-7 (Sigma, CBL271 1:200)

Abs, followed by secondary Ab (ThermoFisher, A-21206; A-32766). Images were taken using fluorescent microscope (Olympus), and analyzed using ImageJ.

shRNA knockdown of TFs in primary mouse HSCs

shRNA-expressing lentiviral plasmids were co-transfected with plasmids pVSV-G and pCMVd8.2 dvpr into 293T cells. Virus containing media were collected 72 h later, filtered (0.22-μm pore size), concentrated by ultracentrifugation, and purified on a sucrose 20% gradient. Viral titers were measured using immunocapture p24-gag ELISA (Sequencing core facility, LJI). For viral transduction, lentiviral vectors at a multiplicity of infection (moi) of 30 + polybrene (10 μg/ml) were added to primary mHSCs (60–70% confluency, 24h after plating) for 36 hours, afterward fresh media containing ± puromycin (5 μg/ml) was added to infected cells for 48 hours. mHSCs were harvested, gene silencing was analyzed by qRT-PCR and RNA-Seq. Multiple shRNA hairpins were tested: ETS1 (n=5), ETS2 (n=10), NF1 (n=4), NF2 (n=5), GATA4 (n=5), GATA6 (n=5), IRF1 (n=7), IRF2 (n=10). A minimum of two target sequences with the least off-target knockdowns was selected for each gene (Suppl. Table 1), compared to non-coding hairpins. Infection with SHC-002 (CTRL1) was used as a control for targeting NF1/2, ETS1/2, GATA4/6 in mHSCs; SHC-202 (CTRL2) was used as a control for targeting IRF1/2 in mHSCs. CTRL1 (−) or CTRL2 (−) corresponds to SHC-002 (or SHC-202)-infected cells without puromycin treatment.

Human HSCs

Primary human HSCs were isolated using the pronase/collagenase method from donor livers declined for transplantation (www.lifesharing.org) for reasons unrelated to liver injury/fibrosis. See supplemental materials for details.

Primary cell culture

Primary mouse and human HSCs were cultured in Dulbecco's modified Eagle's medium (DMEM Life Technologies, 11965–092) supplemented with 10% FBS (Corning, 35–011-CV) and 1% Antibiotic-Antymycotic (Life Technologies #15240–062). mHSCs or hHSCs (0.5×10^5 cells) were stimulated with TGFβ1 (5ng/ml) for 6h, and analyzed by qRT-PCR.

In vivo model of inactivation of human HSCs

hHSCs were *in vitro* stimulated with TGFβ1 (5ng/ml, 24 hours), labeled with PKH26 (Sigma, PKH26GL-1KT). Activated hHSCs were stored in Trizol (1×10^6 cells), or adoptively transferred into the livers of one day old $Rag2^{-/-}$ $\gamma c^{-/-}$ mice (1×10^6 cells/mouse)[1]. Mice were sacrificed 7–14 days later and $PKH26^+$ hHSCs were sort purified. Input and recovered PKH26-labeled hHSCs were analyzed by qRT-PCR.

Results

Gene expression profiling distinguishes qHSC, aHSCs, and iHSCs

$Col1\alpha2^{Cre}$ mice were crossed with $Rosa26^{flox\text{-}Stop\text{-}flox\text{-}YFP}$ reporter mice to generate $Col1\alpha2^{YFP}$ mice. Upon activation, all aHSCs and their progeny were irreversibly labeled by YFP expression in these mice. qHSCs ($YFP^-VitaminA^+$), aHSCs and iHSCs (YFP

$^{+}$VitaminA^{+}) were sort purified[1] from the livers of uninjured, CCl_4-injured (1.5 months) Col1α2^{YFP} mice, or following 10 days or 1 month of CCl_4 cessation[1] (Figure 1A–B), and their gene expression profiles were compared. Activation of HSCs was associated with suppression of PPARγ and GFAP, and induction of Col1α1 and αSMA. Relative to aHSCs, iHSCs downregulated Col1α1 and αSMA, and upregulated PPARγ (but not GFAP), and this gene expression pattern was identified as a key combination of markers associated with HSC inactivation [1].

Phenotypic changes in HSCs were associated with specific patterns of transcription factor (TF) expression

The co-regulated clusters of transcription factors (TFs) and their biological functions were identified in qHSCs, aHSCs, and iHSCs (Figure 1C, Suppl. Figure 1A). The profile of TF expression in qHSCs changed dramatically in response to CCl_4, and was characterized by strong downregulation of quiescence-associated TFs (clusters 1 & 2), and induction of fibrogenic TFs (clusters 4 & 5). In turn, a small number of genes (cluster 6) were transiently expressed in iHSCs after 10 days of CCl_4 cessation, implicating this group of TFs is driving aHSC inactivation. Expression of fibrogenic TFs was suppressed in iHSCs, while expression of quiescence-associated TFs was gradually restored either after 10 days (“quick recovering” genes, cluster 4) or 1 month (“slow recovering” genes, cluster 5, Figure 1C, Suppl. Figure 1A), suggesting that similar transcriptional mechanisms might regulate HSC quiescence and inactivation. Activity of regulatory elements and their target genes is regulated by the epigenome [12]. To evaluate potential mechanisms underlying the phenotypic changes in HSCs, the epigenetic landscape of qHSCs, aHSCs, and iHSCs was examined.

Characteristic changes in the enhancer repertoire distinguish qHSCs, aHSCs, and iHSCs

ChIP-Seq analysis was performed to identify the sequence motifs enriched at promoters and enhancers of mouse HSCs marked by H3K4me2 and H3K27ac. ChIP-Seq experiments generated a total of 54,956 peaks marked by either H3K27ac or H3K4me2, or both marks (Suppl. Figure 1B), and revealed the locations of putative enhancers near key expressed genes in qHSCs, aHSCs, and iHSCs (Suppl. Figure 1C). H3K27ac profiling identified peaks that were largely a subset of H3K4me2 sites, and frequently near genes with higher expression (Suppl. Figure 1D). The HSC-derived epigenetic profiles were distinct from the epigenetic patterns described for whole liver tissue [13] and Kupffer cells [14], consistent with the high purity of the HSC preparations (Suppl. Figure 1E).

Epigenetic changes of regulatory elements of specific genes correlated with their mRNA expression and HSC activation state. For instance, increased levels of H3K27ac near DNA with the AP1 motif (TGACTCA) (Suppl. Figure 1F), a known driver of HSC activation[15], were observed in aHSCs. The H3K27ac mark was also increased in the regulatory elements of the AP1-responsive genes, Col1α1 and Col1α2 genes in aHSCs (Suppl. Figure 1G)[1], indicating that our analysis yielded statistically and biologically significant results.

Differential H3K4me2 binding identified genomic sites corresponding to TFs with high/low transcriptional activity in qHSCs, aHSCs, and iHSCs

Unbiased clustering analysis revealed changes in H3K4me2 levels for each HSC state (Figure 1D). TF motif enrichment cluster analysis identified a candidate TFs that may play critical roles in regulation of HSC phenotypes (Figure 1E). Clusters of enhancers (cluster 1, such as ETS) were strongly repressed in aHSCs (vs qHSCs). Inactivation of HSCs was associated with transcriptional repression of fibrogenic TFs (cluster 4 & 6, such as AP1), and gradual restoration of quiescence-associated TFs in iHSCs after 10 days ("quick recovering", cluster 2) or 1 month ("slow recovering", cluster 1) of CCl_4 cessation (vs qHSCs), while TEAD and IRF motifs were enriched in enhancers transiently activated during recovery (e.g. cluster 5).

Differentially H3K27ac-regulated TFs and their target genes were identified for qHSCs, aHSCs, and iHSCs

Similar hierarchical clustering was performed for H3K27ac patterns and revealed several clusters of dynamically induced regulatory elements of TFs that changed their epigenetic status in a coordinated fashion (Figure 1F). Each cluster was analyzed for enriched DNA motifs and was linked to a specific HSC phenotype. The genes located near the enhancers identified in each cluster shared the same general pattern of expression predicted by the changes in H3K27ac (Figure 1F), and were linked to their enrichment in specific pathways or other biological processes (Figure 1F). Enhancers with high binding of H3K27ac (cluster 4) in aHSCs were highly enriched for AP-1, TEAD, and NF- κB motifs, consistent with their known roles in HSC activation [15]. In contrast, enrichment for ETS, IRF, and FOX motifs (clusters 1, 2, 3) were mostly associated with enhancers that were initially induced in qHSCs, repressed in aHSCs, and then re-expressed at different times in iHSCs, suggesting that the TFs binding these motifs may play a role in the quiescent and inactivated HSC phenotypes (Suppl. Figure 2B).

The genes for ETS1/2, GATA4, and IRF1 are associated with super-enhancers in HSCs

Genome-wide analysis of H3K4me2 and H3K27ac peaks (Figure 2) identified a group of TFs with the highest transcriptional activity in all HSC phenotypes (independent of activation), including ETS, IRF, and GATA (summarized in Figure 2A). Each of these enriched ETS, IRF, and GATA motifs can be potentially bound by large families of TFs (that share a common DNA binding domain), and bind to DNA with similar DNA sequence preferences [16]. To identify which TFs are likely to bind each motif in HSCs and play important functional roles, the H3K27ac ChIP-Seq data were analyzed for the presence of super-enhancers (regions of high enhancer density in the vicinity of genes important for cell identity)[17]. This approach identified 622 super-enhancers, compiled by TF family[18], their gene expression levels were annotated, and the super-enhancer-associations (that discriminates between TF family members that potentially play a role in HSC biology) were determined (Figure 2B). The comparison of normalized gene expression and H3K27ac/H3K4me2 ChIP-seq read densities identified super-enhancers that occur near ETS1 (Figure 2C), IRF1, and GATA4 (Suppl. Figure 2C–D).

ETS1/2, GATA4/6, and IRF1/2 TFs are putative lineage-specific TFs in HSCs

Super-enhancers are often found at key regulators with cell-restricted expression. Lineage determination of specific cell types is often defined by a combination of TFs that tend to co-localize on a genome-wide scale at the sites of accessible chromatin and/or enhancer-like elements [5]. Next, the enhancer repertoires were analyzed for the key TFs responsible for orchestrating HSC cell-lineage functions. The likely binding motifs for these factors were computationally identified by mining the regulatory sequences marked by H3K27ac or H3K4me2 for overrepresented sequences of TF binding sites compared to random genomic sequences that serve as background. The *de novo* motif discovery program HOMER [5] was applied to HSC promoter-distal (>3 kb) regulatory elements, and identified DNA motifs bound by putative lineage determining ETS, IRF, and GATA motifs TFs (Figure 2D). Gene expression profiling was used to determine the mRNA levels of each TF family member (reasoning that the key TFs are more likely to be highly expressed), and identified the following isoforms ETS1, ETS2, IRF1, IRF2, GATA4, and GATA6 as candidate HSC lineage-determining TFs (Figure 2E).

shRNA-knockdown of HSC lineage-determining factors in primary mouse HSCs

To determine the role of the putative lineage-determining factors in HSC biology (Figure 3A), specific shRNA sequences with the highest knockdown efficiency and lowest off target effects (Suppl. Table 1) were selected to knockdown each TF in primary HSCs (Figure 3B–C) (Suppl. Figure 3A). The gene expression profiles of targeted HSCs were compared to control HSCs (infected with non-targeting shRNA-expressing lentiviruses) by qRT-PCR and RNA-Seq (Figure 3B–D). The effect of each individual TF knockdown on expression of ETS1/2, GATA4/6, IRF1/2 was analyzed, and the relationship between TFs was established. Arrows point towards TFs whose expression is downregulated, and the average percent of downregulation is indicated for targeted TFs (Figure 3E). Specifically, shRNA-knockdown of GATA6 resulted in downregulation of GATA4 and ETS1. ETS1 knockdown suppressed expression of ETS2, as well as downregulation of its target genes, NF1 and PPARγ (Figure 3D–E), suggesting that the shRNA-knockdown in targeted HSCs yields biologically relevant results, and is suitable to study functional properties of HSC lineage determining factors.

shRNA-knockdown of HSC lineage-determining factors resulted in activation and a loss of HSC-phenotype

Lineage-determining TFs are implicated in the regulation of cellular homeostasis, viability, and response to injury or stress [5]. When putative HSC lineage-specific TFs were knocked down individually (ETS1, ETS2, GATA4, GATA6, IRF1, or IRF2, Figure 4A & D) or family-wise (ETS1/2, GATA4/6, or IRF1/2, Figure 4B & E), HSCs did not apoptose [5]. Instead, the cells became highly proliferative (along with increased expression of Cdk2, 4 and Ccnd1, Figure 4B), downregulated expression of quiescence-associated genes (PPARγ, Insig1, Figure 4B), and strongly induced expression of fibrogenic (Col1α1, Acta1, TIMP1, Spp1 and LoxL2, Figure 4B) and inflammatory genes (CXCL5, CXCL1, IL-6 and IL-1β Figure 4B). Unexpectedly, we also observed upregulation of epithelial (Epicam, K18, K19, Alb, and HNF1alpha) and progenitor (Afp, Yap1, and Sox9) markers in targeted HSCs,

indicating that knockdown of HSC lineage-determining factors results in a loss of the HSC/mesenchymal phenotype (Suppl. Figure 3A–B).

shRNA-knockdown of GATA4/6 or ETS1/2 is critical for development of activated phenotype in targeted HSCs

We compared gene expression profiles of the shRNA-targeted HSCs and *in vivo*-activated HSCs (sorted from livers of CCl_4-injured Col1α1^{YFP} mice)[1]. Using Gene Set Enrichment Analysis (GSEA) and DESeq2/Metascape unbiased pathway analysis[19], we observed significant correlation between shRNA-knockdown of individual TF (or their families) in targeted HSCs and expression of inflammatory/fibrogenic genes (associated with extracellular matrix proteins, inflammation, and chemotaxis pathways, Figure 4C–D) similar to the gene sets observed in *in vivo* activated HSCs (vs qHSCs, Suppl. Figure 3C–D). Meanwhile, shRNA-knockdown of GATA4/6 and ETS1/2 (but not IRF1/2) was mostly responsible for expression of fibrogenic genes of targeted HSCs, suggesting that these TFs mediate suppression of fibrotic signals in HSC (Figure 4E). The biological role of our targets in HSCs was further evaluated *in vivo*.

Deletion of GATA6 in HSCs accelerates development of liver fibrosis in CCl_4-injured mice

Mice exhibiting HSC-specific ablation of GATA6 (generated by crossing Lrat^{Cre} mice with GATA6-floxed mice) are more susceptible to CCl_4-induced injury than wt littermates (Figure 5A, Suppl. Figure 4A–B), as shown by increased area of Sirius Red and α-SMA staining (Figure 5A), along with upregulation of fibrogenic (↑2 fold α-SMA, Timp1, and Loxl2) and inflammatory (↑2 fold Cxcl5, and IL-6) genes (Figure 5B). Our *in vivo* data are in concordance with our *in vitro* results, suggesting that GATA6 suppresses activation of HSCs. Moreover, regression of liver fibrosis was attenuated in Lrat$^{\Delta GATA6}$ mice compared to wt littermates (2 weeks after CCl_4 cessation, Suppl. Figure 5). Significantly, the fibrosis resolution was 15% less in Lrat$^{\Delta GATA6}$ mice than in wt mice, as demonstrated by persistence of Sirius Red and αSMA, and expression of Col1α1, αSMA, Spp1, and Timp1 mRNA (Suppl. Figure 5). Our data suggest that GATA6 drives inactivation of HSCs.

ETS1 target genes Neurofibromin 1 (NF1) and PPARγ are downregulated in aHSCs

ETS1 is implicated in the maintenance of HSCs in a quiescent-like phenotype [20]. However, tissue-specific ablation of ETS1/2 often results in an embryonic lethal phenotype[7], outlining the importance of these factors for growth and development. Therefore, Lrat$^{ETS1+/-}$ mice, heterozygous for *Ets* gene specifically in HSCs, were generated by crossing Lrat^{Cre} mice with ETS1-floxed mice (Suppl. Figure 4C). Development of CCl_4-induced liver fibrosis was exacerbated in Lrat$^{ETS1+/-}$ mice (wt littermates, Figure 5A), as shown by increased area of Sirius Red and α-SMA staining, and upregulation of fibrogenic (↑1.6 fold Col1α1, 1.3 fold α-SMA, and 1.5 fold desmin) genes (Figure 5C). In accord, ETS1$^{+/-}$ HSCs isolated from CCl_4-injured Lrat$^{ETS1+/-}$ mice exhibit a more activated phenotype, compared to wt aHSCs (Figure 5C). Moreover, HSCs from uninjured mice had a phenotype intermittent between quiescence and activation, since they had upregulated Cola1a (2.5 fold), αSMA (2 fold), and desmin (2 fold) (Suppl. Figure 4C).

To further assess the physiological relevance of ETS1 in HSC biology, the role of ETS1 downstream targets NF1 and PPARγ was evaluated (Figure 3D). Moreover, expression of both PPARγ and NF1 was downregulated in aHSCs, but only PPARγ (but not NF1) was re-expressed in iHSCs during fibrosis resolution (Figure 4F–G).

HSC-specific deletion of Neurofibromin 1 (NF1), a known ETS1 target, accelerates development of liver fibrosis in CCl_4-injured mice

NF1 has been implicated in the pathogenesis of neurofibromatosis, osteogenesis, and tissue fibrosis in mice, and its activity is regulated by ETS1 [21, 22]. $Lrat^{\Delta NF1}$ mice (devoid of NF1 in HSCs) were slightly smaller in size (vs wt littermates), but displayed no hepatic abnormalities until injury (Figure 5A, Suppl. Figure 4D). In response to CCl_4, $Lrat^{\Delta NF1}$ mice developed ≈30% more liver fibrosis than wt littermates, as shown by increased area of Sirius Red and αSMA staining (Figure 5A), and expression of Col1α1 (↑7-fold), αSMA (↑13-fold), Timp1 (↑6-fold), Loxl2 (↑4-fold), and Cxcl5 (↑7-fold, Figure 5D) was upregulated in the livers of CCl_4-injured $Lrat^{\Delta NF1}$ relative to wt mice, indicating that NF1 plays a critical role in preventing HSC activation.

HSC-specific ablation of PPARγ increases susceptibility to CCl_4-induced liver fibrosis and impairs fibrosis resolution in $Lrat^{\Delta PPAR\gamma}$ mice

PPARγ has been implicated in the maintenance of quiescent and inactivated HSC phenotypes in culture[23], but its *in vivo* role in HSCs is unknown. shRNA-knockdown of ETS1 strongly suppressed expression of PPARγ in targeted HSCs, and the PPARγ promoter contains a functional ETS1 binding site (Suppl. Figure 6). Development and regression of liver fibrosis was studied in $Lrat^{\Delta PPAR\gamma}$ mice. Deletion of PPARγ in qHSCs (compared to wt qHSCs, Figure 6A) was associated with downregulation of CEBPδ, Insig1, SREBPα, and ETS1 (Figure 6A). When challenged with CCl_4, $Lrat^{\Delta PPAR\gamma}$ mice developed ≈40% more fibrosis than wt littermates (Figure 6B–C). Moreover, the rate of fibrosis resolution was ≈30% slower in $Lrat^{\Delta PPAR\gamma}$ mice than in wt mice (1 month after CCl_4 cessation), as demonstrated by persistence of Sirius Red staining and expression of Col1α1 and αSMA mRNA (Figure 6B–C). Together, these results suggest that expression of PPARγ in HSCs is critical for the maintenance of quiescent and inactivated phenotypes.

PPARγ agonist drives inactivation of HSCs and accelerates regression of liver fibrosis in wt mice

Administration of the PPARγ agonist rosiglitazone (5 mg/kg, daily, gavage) accelerated regression of liver fibrosis in CCl_4-injured wt mice and was associated with increased expression of PPARγ and downregulation of Col1α1, αSMA, TIMP1, and Spp1 mRNA (vs vehicle-treated wt mice, Figure 6D–F). Remarkably, rosiglitazone had little effect on resolution of CCl_4-induced fibrosis in $Lrat^{\Delta PPAR\gamma}$ mice (Figure 6G), demonstrating that PPARγ signaling specifically in HSCs is critical for HSC inactivation. In support, *in vitro* administration of rosiglitazone (20 μM) effectively suppressed Col1α1 expression in TGFβ1-stimulated wt HSCs, as well as in NF1-deficient HSCs (which are prompt to activate), suggesting that activating PPARγ can facilitate inactivation of HSCs (Figure 6H).

Human aHSCs can inactivate *in vivo*

Similar to mouse HSCs, human HSCs can inactivate into a quiescent-like state (iHSCs) *in vivo* when placed into an environment that does not support fibrogenic stimuli (Figure 7A). For this purpose, primary PKH26-labeled human HSCs (Suppl. Figure 7A–B) were *in vitro* stimulated with TGF-β1 (5 ng/ml), and adoptively transplanted into the livers of 1 day- old $Rag2^{-/-}\gamma c^{-/-}$ pups[1]. After 7 or 14 days, livers were analyzed by immunohistochemistry for $PKH26^{+}Desmin^{+}$ HSCs (Figure 7A), and engrafted human $PKH26^{+}$ HSCs were sorted, and analyzed using qRT-PCR. Compared with the input aHSCs, the recovered HSCs down-regulated Col1α1 and α-SMA and up-regulated PPARγ mRNA. Thus, in the normal liver environment, human aHSCs can inactivate into a quiescent-like phenotype (Figure 7B).

ChIP-Seq analysis identifies active regulatory regions in human HSCs

The analysis of human HSC H3K27ac and H3K4me2 ChIP-seq data revealed 85,110 peaks marked by one or both epigenetic modifications (Suppl. Figure 7C). The epigenetic profiles of human HSCs were distinct from profiles generated from human whole liver [24] (Suppl. Figure 7D), yet were highly similar to published human HSC DNase I hypersensitivity mapping [25] and H3K27ac data from human myofibroblasts [26] (Suppl. Figure 7E). Furthermore, H3K27ac and H3K4me2 epigenetic marks from human HSCs were highly enriched at HSC promoter-distal DNase I hypersensitive peaks compared to H3K27ac and H3K4me2 levels from human whole liver, further demonstrating that our profiles capture HSC-specific epigenetic signals (Suppl. Figure 7F). Next, we compared human and mouse H3K4me2 and H3K27ac peaks across orthologous regions of their genomes, finding that roughly 50% of active regulatory elements in mouse were also active in human (Figure 7C), which is consistent with cross-species conservation of regulatory elements in other tissues[27].

ETS1, IRF2, and GATA6 are putative lineage-specific TFs in hHSCs

The *de novo* motif discovery program HOMER identified HSC promoter-distal (>3 kb) regulatory elements that were highly enriched with motifs for AP-1, TEAD, ETS, FOX, IRF, and GATA families of TFs (Figure 7C). Additional motifs for the AP-1 and TEAD TF families were enriched in human HSC enhancers (Figure 7D–E), reflecting the activation of enhancers in cultured human HSCs [28]. The ETS1 locus was located within one of the 506 super-enhancers identified in human HSCs by directly analyzing human HSC H3K27ac ChIP-Seq data (Figure 7E). Similar to mouse HSCs, ETS, IRF, and GATA were identified as candidates for lineage-determining TFs in human HSCs (Figure 7C), indicating that the HSC epigenetic signature is highly preserved in humans and mice. In support of our findings, the identified motifs were likely to be bound by TFs, as predicted by the analysis of human DNase I hypersensitivity data generated by the Encode consortium[25] (Suppl. Figure 7G). In further support of our findings, expression levels of ETS1 and its target gene NF1 were upregulated in human HSCs isolated from normal livers, but downregulated in HSCs from patients with NASH and ALD (Suppl. Figure 7H).

Administration of a PPARγ agonist prevents TGF-β1-induced activation of human HSCs

We tested whether a PPARγ agonist can prevent/revert activation of human HSCs. *In vitro* stimulation of human HSCs with TGF-β1 (5 ng/ml) resulted in a rapid upregulation of

fibrogenic genes (Col1α1, Acta2, LoxL2, and TGFβ1), and downregulation of PPARγ mRNA, (Figure 7F). Pretreatment with rosiglitazone (20 μM) prevented TGF-β1-induced activation and Col1α1 expression in human HSCs (Figure 7G), demonstrating the role of PPARγ in maintaining a quiescent phenotype in human HSCs.

DISCUSSION

Hepatic Stellate Cells (HSCs) possess remarkable plasticity (e.g., differentiate from quiescent to activated, and back to inactivated phenotypes), which makes them an attractive target for antifibrotic therapy. We compared gene expression profiles with an epigenetic analysis of H3K4me2 and H3K27ac marks, and identified a unique combination of ETS1/2, GATA4/6, and IRF1/2 as putative HSC lineage-determining transcription factors that are uniquely expressed in HSCs compared to other cells. These TFs play a critical role in the maintenance of the quiescent-like HSC phenotype, as shown by *in vitro* shRNA-knockdown of each TF or their families, and further supported by *in vivo* HSC-specific genetic ablation in mice of *GATA6* and of the ETS1 target genes *NF1* and *PPARγ*. Evidence for similar mechanisms was identified in human HSCs. Similar to mouse HSCs, activation of human HSCs is regulated by ETS, GATA, IRF, and the ETS-target genes NF1 and PPARγ.

Since *in vitro* models may not recapitulate the *in vivo* conditions, new experimental models to study HSC inactivation are needed. We have developed a novel *in vivo* approach to study activation and inactivation of human primary HSCs. Adoptively transferred human HSCs engraft and proliferate in the livers of immunodeficient $Rag2^{-/-}\gamma c^{-/-}$ mice. Moreover, when TGF-β1-activated human aHSCs were placed into this physiological environment lacking fibrogenic stimuli, they downregulated expression of fibrogenic genes and re-acquired expression of PPARγ. Similar to mouse iHSCs, human iHSCs can be identified as Vitamin $A^{+}Col1\alpha1^{low}\alpha\text{-}SMA^{low}GFAP^{low}PPAR\gamma^{hi}$ HSCs. For the first time, we provide evidence that human HSCs can undergo inactivation *in vivo*, suggesting that inactivation of human HSCs may become a novel strategy to halt liver fibrosis/cirrhosis in patients.

Our study identified HSC lineage-specific TFs in mouse and human HSCs. Epigenetic alterations[12] were implicated in driving activation of quiescent HSCs into aHSCs/myofibroblasts[15]. Conversely, transcriptional activity of ETS1 [20] and PPARγ[23] were linked to a quiescent HSC phenotype. In concordance with previous reports, our study identified AP1, Mef2, STAT, NF-κB, TEAD, SOX, and FOX TFs as key regulators of HSC activation, while ETS and GATA TFs were associated with quiescent and inactivated HSC phenotypes. Furthermore, a particular combination of ETS1/2, GATA4/6, and IRF1/2 TFs was uniquely expressed in HSCs, and may be considered as putative HSC lineage-determining factors that cooperatively act to preserve HSC lineage identity. Other TFs were less abundant in HSCs, and therefore were not tested in this study.

Lineage-determining TFs have been identified for macrophages, hepatocytes, and several other cell types [5, 29]. For example, *in vitro* ablation of PU.1, a critical regulator of macrophage differentiation (and a member of ETS family of TFs) resulted in macrophage apoptosis [5]. Surprisingly, *in vitro* shRNA-knockdown of the putative HSC lineage-specific TFs (GATA4/6, ETS1/2 and IRF1/2) did not cause apoptosis (Suppl. Figure 2A), but rather

increased proliferation, activation, and a loss of HSC-specific phenotype (characterized by the upregulation of epithelial/hepatocyte-specific markers Epicam, CK18, CK19, Alb, Afp, Sox9, HNF1alpha).

Although the mesenchymal origin of HSCs has been well characterized [30], several lines of evidence suggest that HSCs possess unusual plasticity [31], and upon overexpression of a minimal combination of hepatocyte-lineage factors (Foxa3, GATA4 and HNF1alpha), can be *in vivo* trans-differentiated into functional hepatocytes [32]. GATA4 was also shown to play a critical role in HSC activation [6], suggesting that the combination of cell-specific TFs might critically affect HSC cellular fate and responses to stress.

GATA, ETS, and IRF TF families often possess oncogenic activities. However, *in vivo* ablation of GATA4 or GATA6 in mesenchymal cells/HSCs did not yield malignant phenotype in $G2^{GATA4-/-}$ mice [6] or $Lrat^{\Delta GATA6}$ mice, but increased susceptibility of these mice to liver fibrosis. Moreover, suppression of ETS1 was associated with upregulation of fibrogenic genes and rapid HSC activation [20]. In agreement, our study links ETS1 to the regulation of anti-fibrotic properties of HSCs. We identified NF1 and PPARγ as ETS1 target genes that prevent HSC activation. NF1 was originally identified as a tumor suppressor, and mutations of the *NF1* gene cause of neurofibromatosis type 1, as well as skeletal abnormalities [33]. Here we demonstrate that NF1-deficient HSCs were prompt to activate and proliferate, and development of CCl_4-induced liver fibrosis was exacerbated in $Lrat^{\Delta NF1}$ mice.

We and others [1, 23] have proposed a critical role for PPARγ in the regulation of quiescent and inactivated HSC phenotypes. Expression of PPARγ is negatively controlled in HSCs via MeCP2- and EZH2-dependent transcriptional repression of the PPARγ promoter [34]. Our study describes a new ETS1-PPARγ signaling pathway that positively regulates PPARγ expression in qHSCs, and demonstrates that genetic ablation of PPARγ in HSCs *in vivo* promotes the development but inhibits the regression of CCl_4-induced liver fibrosis. Furthermore, we demonstrate that GATA6-deficient HSCs exhibit a defect in inactivation, suggesting that GATA6 and PPARγ agonists can be used to drive inactivation of aHSCs/myofibroblasts and could be assessed as part of a combination strategy to halt liver fibrosis in patients.

Supplementary Material

Refer to Web version on PubMed Central for supplementary material.

Acknowledgments

Grant support: Supported by the National Institutes of Health *R01DK101737, U01AA022614, and R01DK099205, R01DK111866* (T.K.), *R01DK101737, U01AA022614, R01DK09920, P50AA011999, AI043477* (D.A.B.); and *Herman Lopata* Memorial Hepatitis Postdoctoral ALF Fellowship (J.X.)

Abbreviations

qHSCs	quiescent Hepatic Stellate Cells

aHSCs	activated Hepatic Stellate Cells
iHSCs	inactivated Hepatic Stellate Cells
ECM	extracellular matrix
CCl_4	carbon tetrachloride
Col1α1	collagen α1(I)
α-SMA	α-smooth muscle actin
GFAP	glial fibrillar acidic protein
TGFβ1	transforming growth factor beta
PPARγ	peroxisome proliferator-activated receptor gamma
TIMP1	tissue inhibitor of metalloproteinase 1
TF	transcription factor
ETS1 and 2	the E26 transcription-specific TFs 1 and 2
GATA4 and 6	zinc-finger TFs also termed GATA-binding factor 4 and 6
IRF1 and 2	Interferon regulatory factor 1 and 2

REFERENCES

1. Kisseleva T, Cong M, Paik Y, et al. Myofibroblasts revert to an inactive phenotype during regression of liver fibrosis. Proc Natl Acad Sci U S A 2012;109:9448–53. [PubMed: 22566629]
2. Iredale JP, Benyon RC, Pickering J, et al. Mechanisms of spontaneous resolution of rat liver fibrosis. Hepatic stellate cell apoptosis and reduced hepatic expression of metalloproteinase inhibitors. J Clin Invest 1998;102:538–49. [PubMed: 9691091]
3. Troeger JS, Mederacke I, Gwak GY, et al. Deactivation of hepatic stellate cells during liver fibrosis resolution in mice. Gastroenterology 2012;143:1073–83 e22. [PubMed: 22750464]
4. Heintzman ND, Stuart RK, Hon G, et al. Distinct and predictive chromatin signatures of transcriptional promoters and enhancers in the human genome. Nat Genet 2007;39:311–8. [PubMed: 17277777]
5. Heinz S, Benner C, Spann N, et al. Simple combinations of lineage-determining transcription factors prime cis-regulatory elements required for macrophage and B cell identities. Mol Cell 2010;38:576–89. [PubMed: 20513432]
6. Delgado I, Carrasco M, Cano E, et al. GATA4 loss in the septum transversum mesenchyme promotes liver fibrosis in mice. Hepatology 2014;59:2358–70. [PubMed: 24415412]
7. Dittmer J The biology of the Ets1 proto-oncogene. Mol Cancer 2003;2:29. [PubMed: 12971829]
8. Mederacke I, Hsu CC, Troeger JS, et al. Fate tracing reveals hepatic stellate cells as dominant contributors to liver fibrosis independent of its aetiology. Nat Commun 2013;4:2823. [PubMed: 24264436]
9. Zook EC, Ramirez K, Guo X, et al. The ETS1 transcription factor is required for the development and cytokine-induced expansion of ILC2. J Exp Med 2016;213:687–96. [PubMed: 27069114]
10. Zhu Y, Romero MI, Ghosh P, et al. Ablation of NF1 function in neurons induces abnormal development of cerebral cortex and reactive gliosis in the brain. Genes Dev 2001;15:859–76. [PubMed: 11297510]

11. Langmead B, Salzberg SL. Fast gapped-read alignment with Bowtie 2. Nat Methods 2012;9:357–9. [PubMed: 22388286]
12. Page A, Paoli P, Moran Salvador E, et al. Hepatic stellate cell transdifferentiation involves genome-wide remodeling of the DNA methylation landscape. J Hepatol 2016;64:661–73. [PubMed: 26632634]
13. Yue F, Cheng Y, Breschi A, et al. A comparative encyclopedia of DNA elements in the mouse genome. Nature 2014;515:355–64. [PubMed: 25409824]
14. Lavin Y, Winter D, Blecher-Gonen R, et al. Tissue-resident macrophage enhancer landscapes are shaped by the local microenvironment. Cell 2014;159:1312–26. [PubMed: 25480296]
15. Mann J, Mann DA. Transcriptional regulation of hepatic stellate cells. Adv Drug Deliv Rev 2009;61:497–512. [PubMed: 19393271]
16. Weirauch MT, Yang A, Albu M, et al. Determination and inference of eukaryotic transcription factor sequence specificity. Cell 2014;158:1431–1443. [PubMed: 25215497]
17. Whyte WA, Orlando DA, Hnisz D, et al. Master transcription factors and mediator establish super-enhancers at key cell identity genes. Cell 2013;153:307–19. [PubMed: 23582322]
18. Lambert SA, Jolma A, Campitelli LF, et al. The Human Transcription Factors. Cell 2018;175:598–599. [PubMed: 30290144]
19. Subramanian A, Tamayo P, Mootha VK, et al. Gene set enrichment analysis: a knowledge-based approach for interpreting genome-wide expression profiles. Proc Natl Acad Sci U S A 2005;102:15545–50. [PubMed: 16199517]
20. Knittel T, Kobold D, Dudas J, et al. Role of the Ets-1 transcription factor during activation of rat hepatic stellate cells in culture. Am J Pathol 1999;155:1841–8. [PubMed: 10595913]
21. Yang G, Khalaf W, van de Locht L, et al. Transcriptional repression of the Neurofibromatosis-1 tumor suppressor by the t(8;21) fusion protein. Mol Cell Biol 2005;25:5869–79. [PubMed: 15988004]
22. Woods DB, Ghysdael J, Owen MJ. Identification of nucleotide preferences in DNA sequences recognised specifically by c-Ets-1 protein. Nucleic Acids Res 1992;20:699–704. [PubMed: 1542566]
23. She H, Xiong S, Hazra S, et al. Adipogenic transcriptional regulation of hepatic stellate cells. J Biol Chem 2005;280:4959–67. [PubMed: 15537655]
24. Roadmap Epigenomics C, Kundaje A, Meuleman W, et al. Integrative analysis of 111 reference human epigenomes. Nature 2015;518:317–30. [PubMed: 25693563]
25. Thurman RE, Rynes E, Humbert R, et al. The accessible chromatin landscape of the human genome. Nature 2012;489:75–82. [PubMed: 22955617]
26. Zhou C, York SR, Chen JY, et al. Long noncoding RNAs expressed in human hepatic stellate cells form networks with extracellular matrix proteins. Genome Med 2016;8:31. [PubMed: 27007663]
27. Villar D, Berthelot C, Aldridge S, et al. Enhancer evolution across 20 mammalian species. Cell 2015;160:554–66. [PubMed: 25635462]
28. Gosselin D, Skola D, Coufal NG, et al. An environment-dependent transcriptional network specifies human microglia identity. Science 2017;356.
29. Shen Y, Yue F, McCleary DF, et al. A map of the cis-regulatory sequences in the mouse genome. Nature 2012;488:116–20. [PubMed: 22763441]
30. Asahina K, Tsai SY, Li P, et al. Mesenchymal origin of hepatic stellate cells, submesothelial cells, and perivascular mesenchymal cells during mouse liver development. Hepatology 2009;49:998–1011. [PubMed: 19085956]
31. Omenetti A, Yang L, Li YX, et al. Hedgehog-mediated mesenchymal-epithelial interactions modulate hepatic response to bile duct ligation. Lab Invest 2007;87:499–514. [PubMed: 17334411]
32. Rezvani M, Espanol-Suner R, Malato Y, et al. In Vivo Hepatic Reprogramming of Myofibroblasts with AAV Vectors as a Therapeutic Strategy for Liver Fibrosis. Cell Stem Cell 2016;18:809–16. [PubMed: 27257763]

33. Wu X, Estwick SA, Chen S, et al. Neurofibromin plays a critical role in modulating osteoblast differentiation of mesenchymal stem/progenitor cells. Hum Mol Genet 2006;15:2837–45. [PubMed: 16893911]

34. Mann J, Chu DC, Maxwell A, et al. MeCP2 controls an epigenetic pathway that promotes myofibroblast transdifferentiation and fibrosis. Gastroenterology 2010;138:705–14, 714 e1–4. [PubMed: 19843474]

What you need to know

BACKGROUND AND CONTEXT

During liver injury, quiescent hepatic stellate cells (HSCs) become activated into collagen type I-producing myofibroblasts, which promote fibrogenesis. Upon cessation of liver injury, these cells become inactivated and fibrosis can regress.

NEW FINDINGS

We identified lineage-specific transcription factors that regulate activation of mouse and human HSCs. Disruption of these factors increased the severity of chemical-induced liver fibrosis in mice.

LIMITATIONS

This study was performed in mice and with human cells.

IMPACT

We identified transcription factors required for activation and inactivation of mouse and human HSCs. We identified transcriptional and epigenetic regulators of HSC phenotypes, which might be targeted for treatment of liver fibrosis.

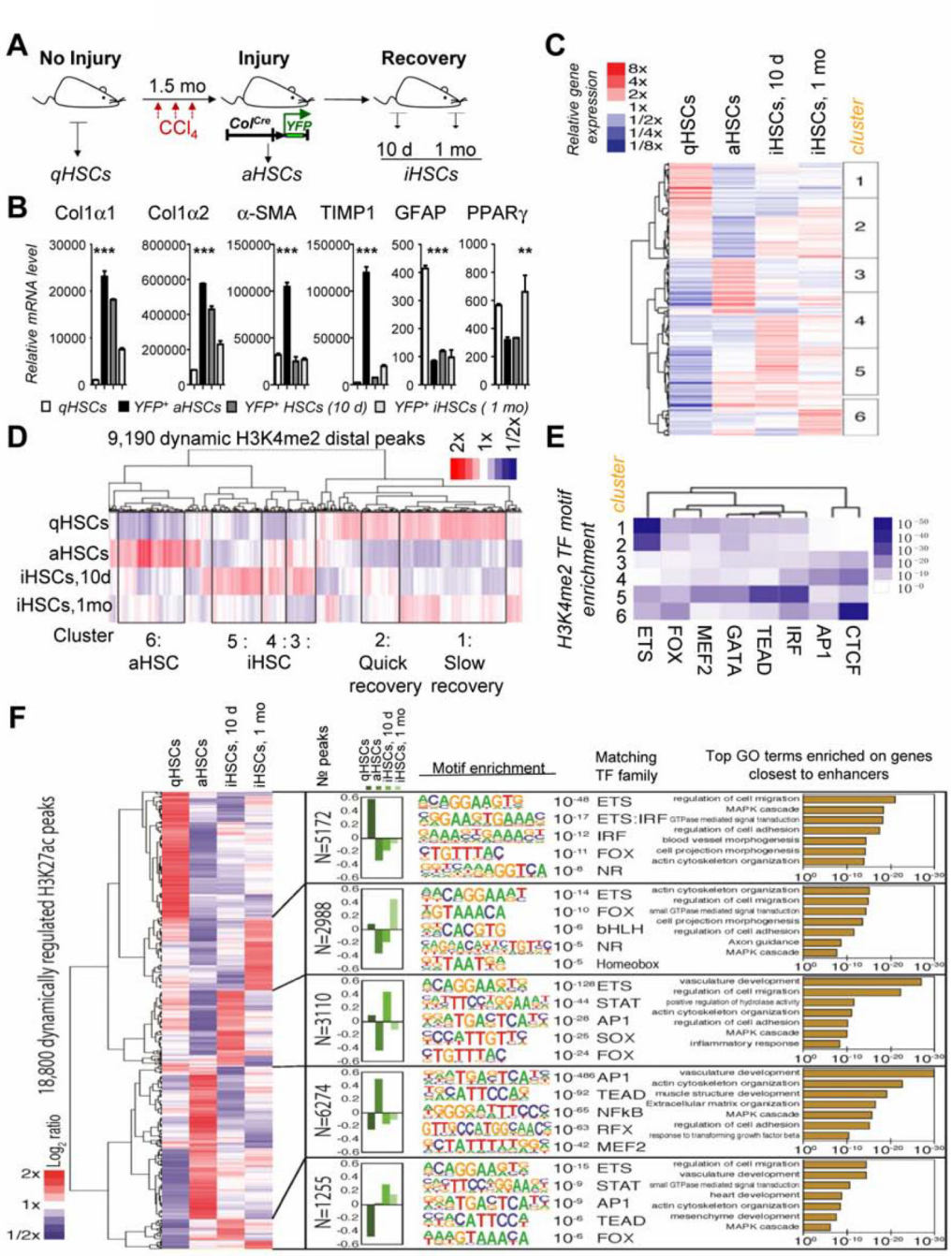

Figure 1. Gene expression profiling and ChIP-Seq analysis of qHSCs, aHSCs, and iHSCs.

(A) qHSCs, aHSCs, iHSCs were sort purified from livers of Col1α2^{YFP} mice and subjected to gene expression microarray.

(B) Expression of selected genes is shown.

(C) Heatmap displaying relative expression of transcription factor (TF) mRNA levels depending on activation status of HSCs.

(D-F) qHSCs, aHSCs, iHSCs were sort purified from livers of Col1α1^{YFP} mice and subjected to gene expression microarray. ChIP-Seq analysis of (10 d and 1 mo): (**D**)

Heatmap and clustering analysis of relative changes in H3K4me2 levels at H3K4me2 promoter-distal peaks. Clusters 1–6-mark major clusters of H3K4me2 peaks with clear regulatory patterns.

(E) Heatmap depicting the relative TF motif enrichment at H3K4me2 peaks (± 500 bp) associated with each of the clusters from (D) relative to random genomic regions.

(F) Heatmap displaying clustering analysis of the dynamic regulation of H3K27ac-defined enhancers, showing the relative changes in H3K27ac levels, the top five TFs enriched at enhancers in the cluster, and the most enriched pathways associated with the genes located closest to the enhancers defined in each cluster.

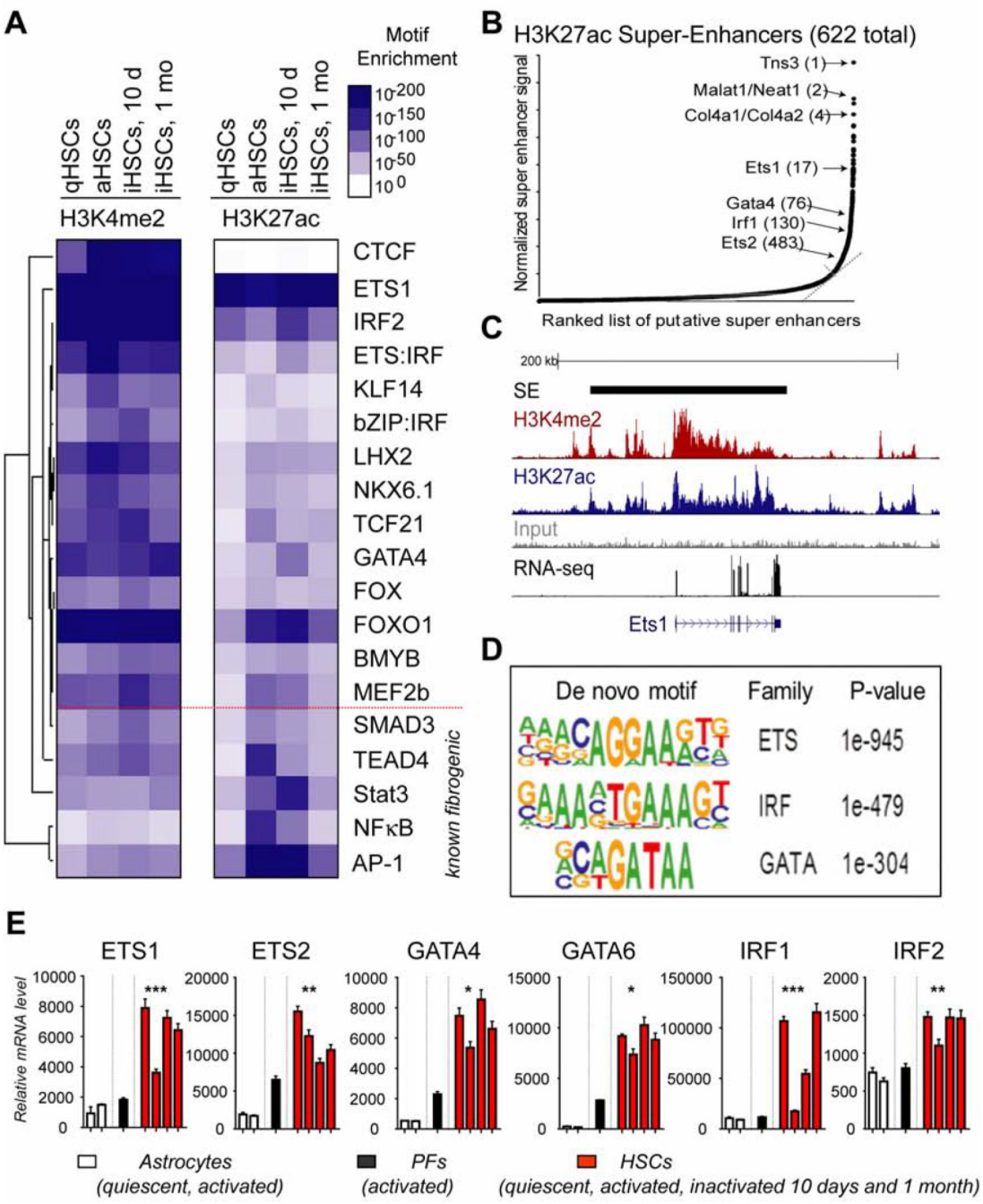

Figure 2. Analysis of H3K4me2 and H3K27ac binding sites identified HSC lineage-specific TFs in mouse HSCs.

(A) Heatmap showing clustering analysis of the top 20 TF motifs enriched at the most-changing H3K4me2- and H3K27ac-marked genomic locations in qHSCs, aHSCs, and iHSCs (10 d and 1 mo).

(B) Super enhancer plot depicting the normalized level of H3K27ac signal at enhancers relative to the enhancer rank (sorted by H3K27ac levels, super enhancers defined where the

slope exceeds a value of 1). Super enhancers found near key genes or transcription factors are indicated with the rank of the super enhancer in parentheses.

(C) H3K4me2 and H3K27ac signal at the ETS1 gene/super-enhancer in HSCs.

(D) Sequence logos corresponding to enriched sequence elements of HSC lineage-specific TFs identified by *de novo* motif analysis (enriched over background $>10^{-100}$).

(E) mRNA expression of HSC lineage-specific TFs in Astrocytes activated Portal Fibroblasts (PFs), and HSCs ($p<0.05$).

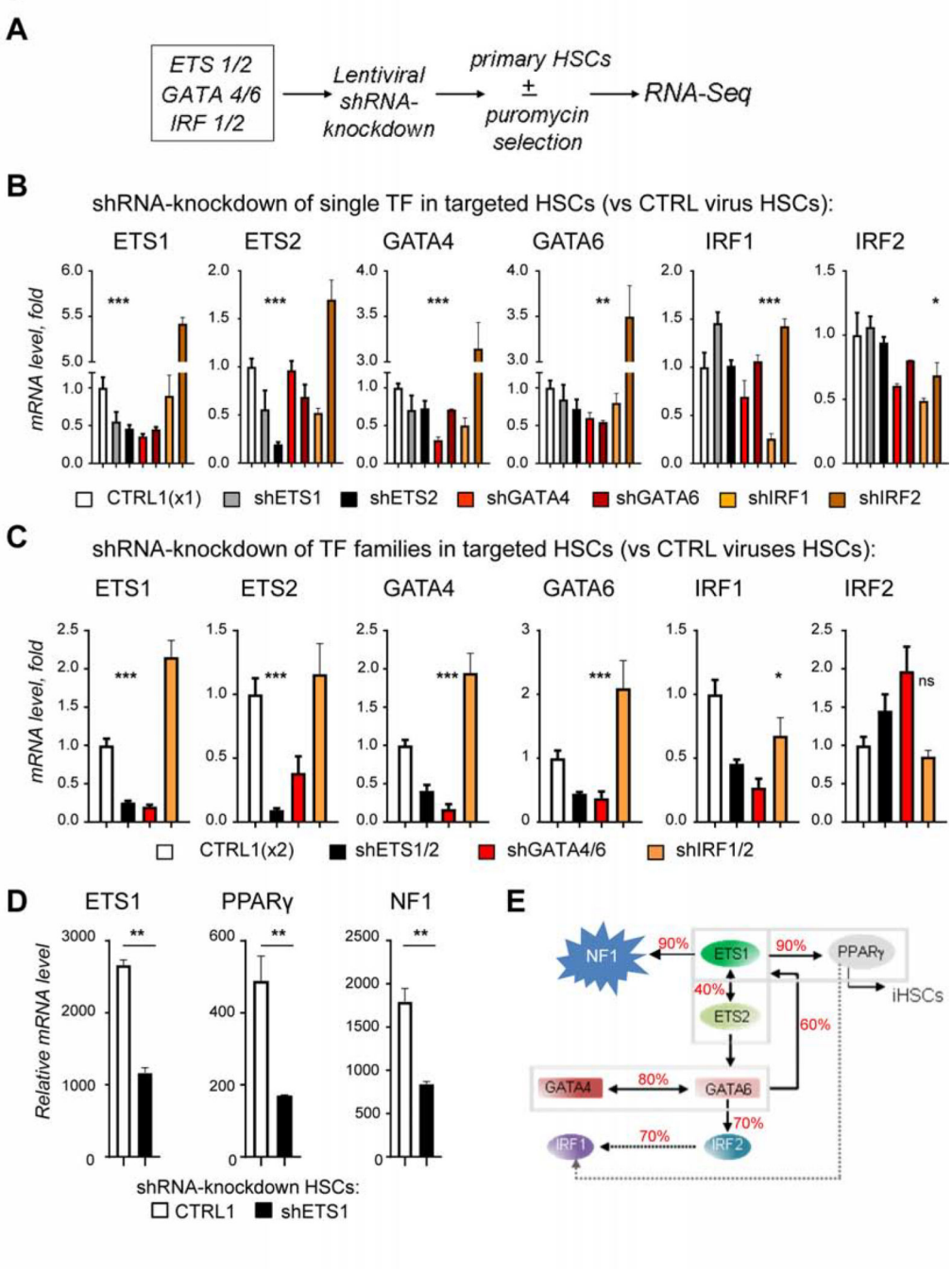

Figure 3. shRNA-knockdown of putative lineage-specific TFs and relationship.

(A) Primary HSCs (1×10^6 cells) were infected with TF-specific shRNA- or non-targeting lentiviruses, followed by ± puromycin (5μg/ml) selection. >2 targeted and control vectors were tested). The data are representative of > 3 independent experiments, $p<0.03$ (see Table 1, see Suppl. Table 2).

(B-C) qRT-PCR of gene expression of targeted HSCs, in which (**B**) individual HSC lineage-determining TF (**C**) or their families were shRNA-knocked down (vs CTRL1, infected with

x 1 or x 2 non-coding viruses). mRNA expression of targeted HSCs was compared to control HSCs, * $p < 0.05$, ** $p < 0.01$, *** $p < 0.001$, student's One-way ANOVA.

(D) RNA-Seq: expression of selected genes in ETS1-knockdown HSCs (vs CTRL1), * $p < 0.05$, ** $p < 0.01$, *** $p < 0.001$, student's *t* test.

(E) Cross regulation between TFs (is based on the combined qRT-PCR/RNA-Seq analysis of the TF expression in targeted HSCs, **(B-C, E)** fold change, * $p < 0.05$, ** $p < 0.01$, *** $p < 0.001$, student's One-way ANOVA.

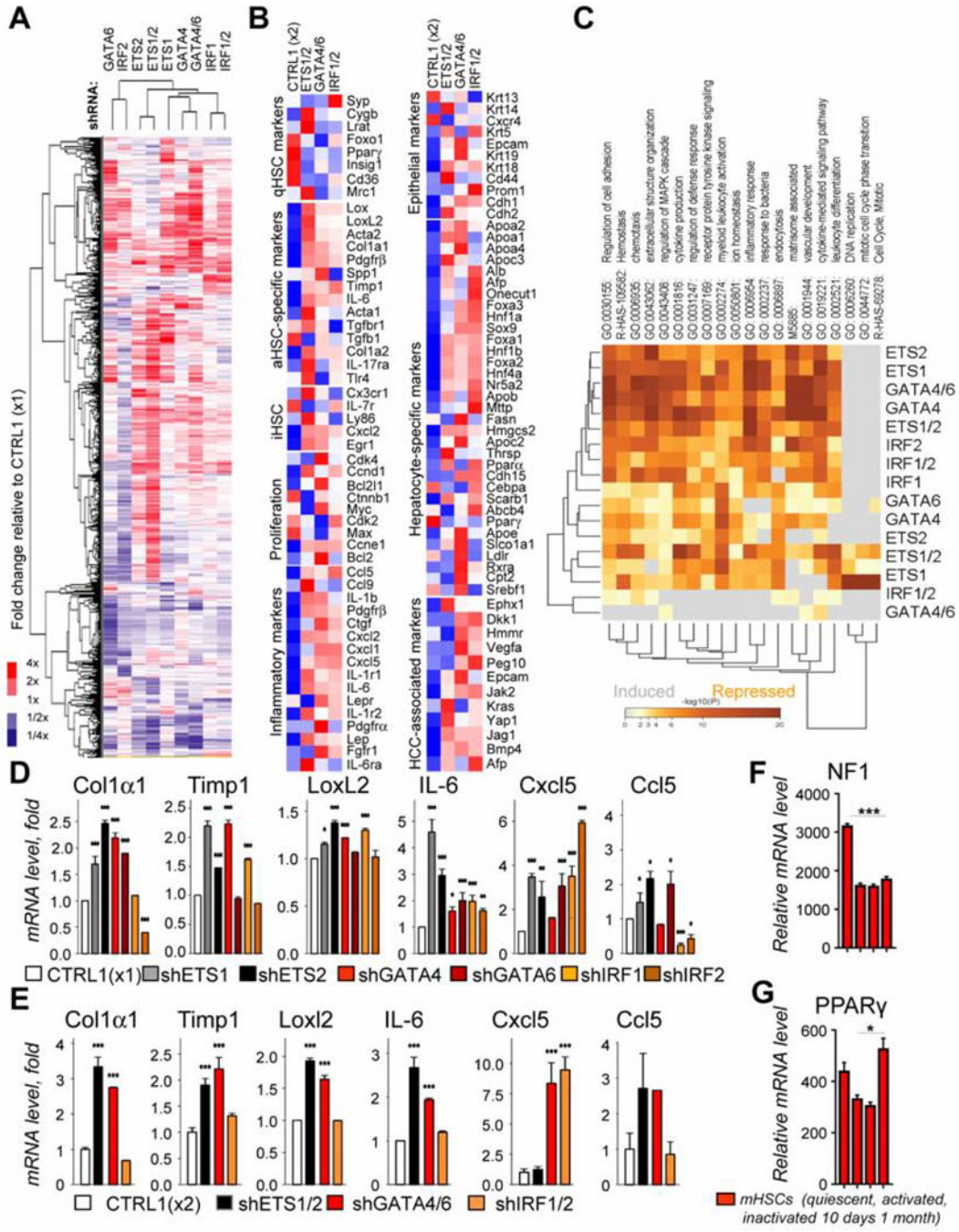

Figure 4. shRNA-knockdown of putative lineage-specific TFs and their families caused over-activation of targeted HSCs.

(A-B) RNA-Seq-based heatmap analysis of expression of **(A)** all genes (arranged in rows by hierarchical clustering), or **(B)** selected genes in shRNA-targeted HSCs (vs CTRL1). Relative expression HSC function-specific genes are shown.

(C) Gene Ontology/Pathway enrichment across sets of genes either induced (grey) or repressed (yellow) by shRNA targeting of key TFs or their families (vs CTRL1) was performed using Metascape software.

(D-E) Expression of fibrogenic/inflammatory genes in targeted HSCs, in which each individual HSC lineage-determining TF **(D)** or their families **(E)** were shRNA-knocked down (vs CTRL1).

(F-G) Expression of NF1 and PPARγ in HSCs (Whole Mouse Genome Microarray, * $p < 0.05$, ** $p < 0.01$, *** $p < 0.001$, student's One-way ANOVA).

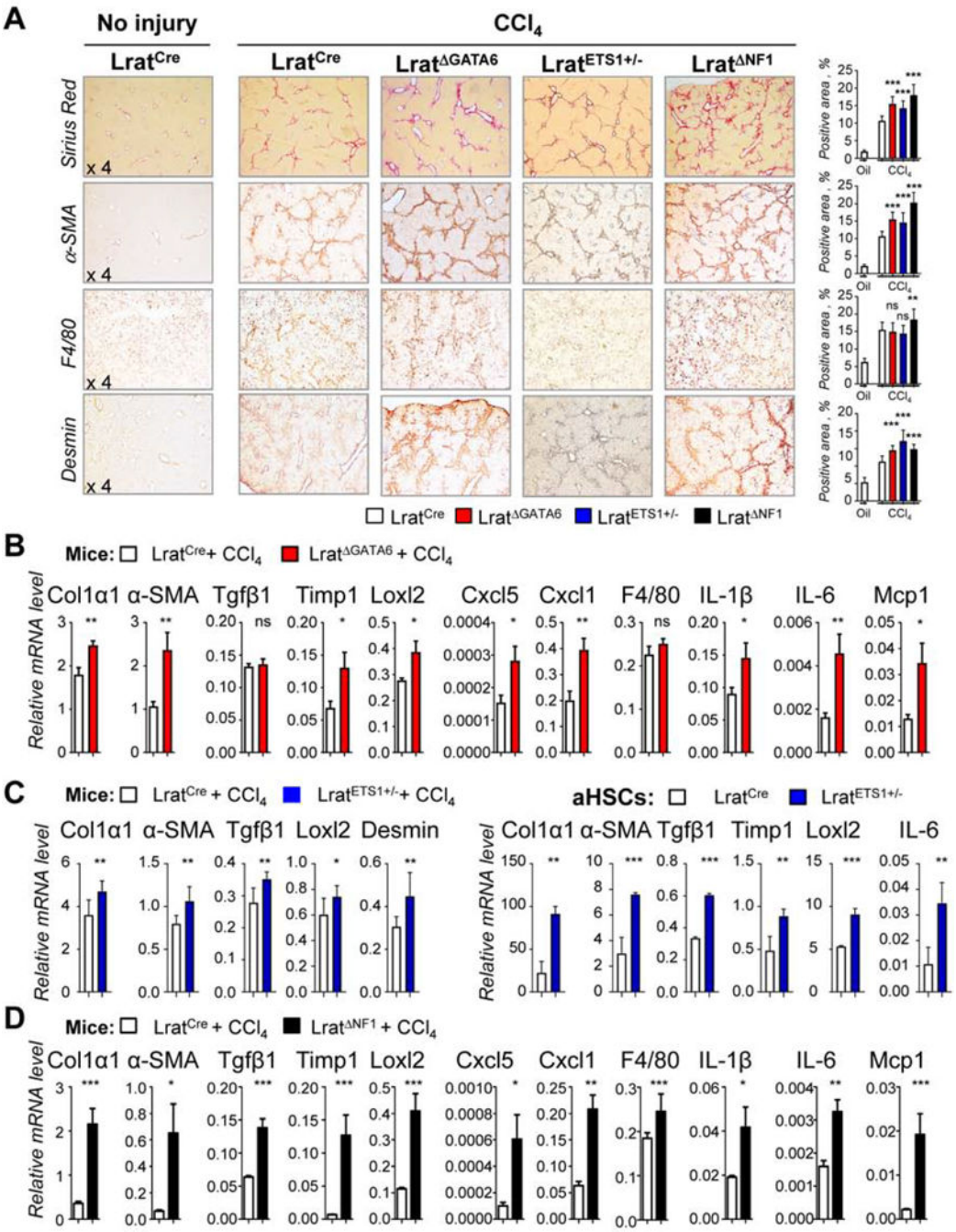

Figure 5. Deletion of GATA6, ETS1$^{+/-}$ and NF1 in HSCs exacerbates development of liver fibrosis in CCl_4-injured Lrat$^{\Delta GATA6}$, Lrat$^{ETS1+/-}$and Lrat$^{\Delta NF1}$ mice.

(A) Livers from uninjured or CCl_4-injured Lrat^{Cre}, Lrat$^{\Delta GATA6}$, Lrat$^{ETS1+/-}$ and Lrat$^{\Delta NF1}$ mice (n=8–12/group) were analyzed by immunohistochemistry, representative micrographs (x 4 objective), positive area was quantified as percent.

(B-D) Livers from **(B)** Lrat^{Cre} and Lrat$^{\Delta GATA6}$, **(C)** livers and aHSCs from Lrat^{Cre} and Lrat$^{ETS1+/-}$, **(D)** Lrat^{Cre} and Lrat$^{\Delta NF1}$ were analyzed by qRT-PCR, * $p < 0.05$, ** $p < 0.01$, *** $p < 0.001$, student's *t* test.

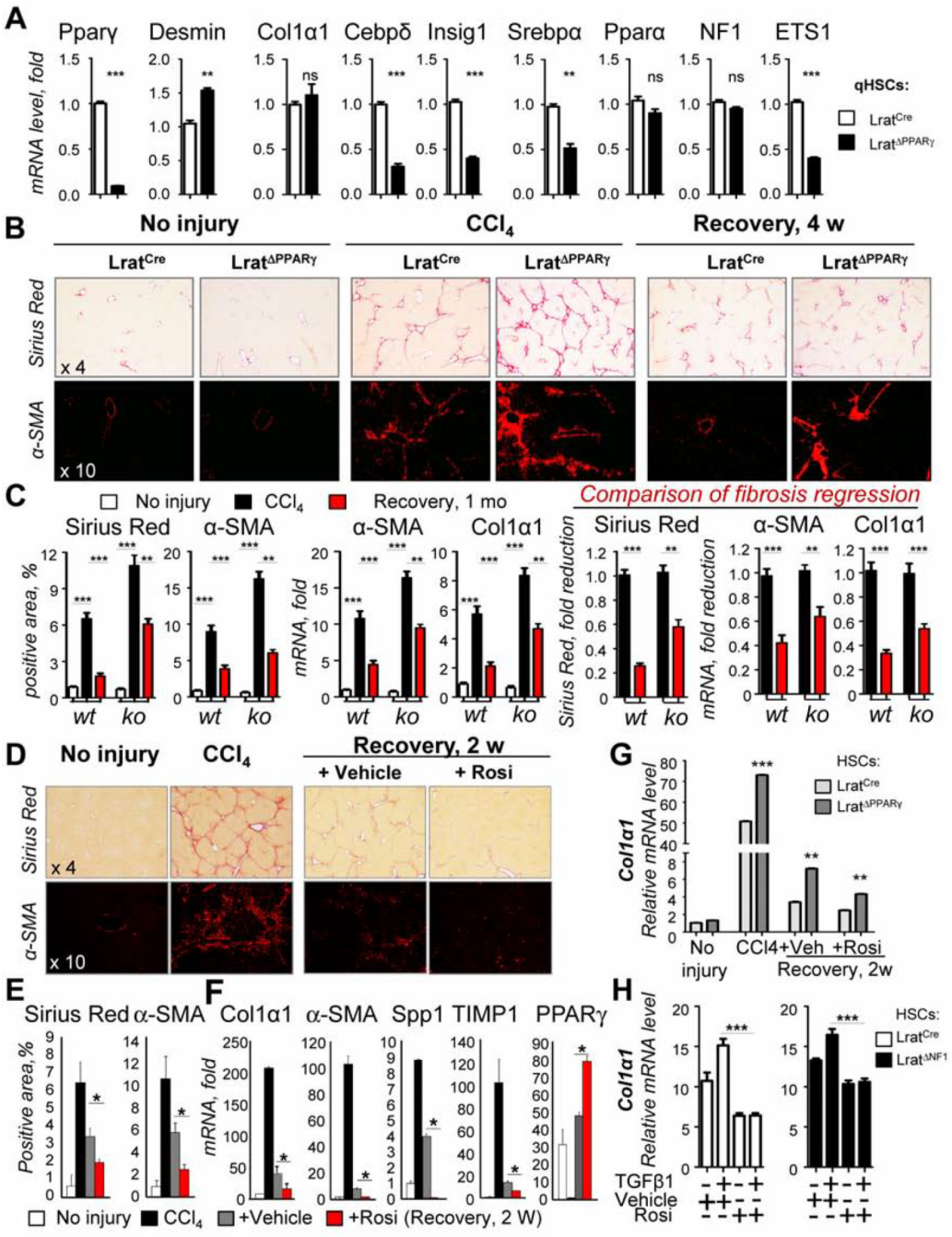

Figure 6. Deletion of PPARγ in HSCs facilitates development of liver fibrosis and prevents fibrosis regression in Lrat$^{\Delta PPAR\gamma}$ mice.

(A) qHSC isolated from Lrat^{Cre} and Lrat$^{\Delta PPAR\gamma}$ mice were analyzed by qRT-PCR. * $p < 0.05$, ** $p < 0.01$, *** $p < 0.001$, student's *t* test.

(B) Livers from Lrat^{Cre} (wt) and Lrat$^{\Delta PPAR\gamma}$ mice (n=8–12/group), uninjured, CCl_4-injured, or after CCl_4 cessation (1 mo) analyzed by immunohistochemistry (micrographs x 4, and x 10 objectives);

(C) Positive staining areas were quantified. Livers were analyzed by qRT-PCR.

(D) CCl_4-injured wt mice (C57Bl/6, n=8–12/group) were treated with rosiglitazone (5 mg/kg, daily) or vehicle for 2 weeks after CCl_4 cessation.
(E) Livers were analyzed by immunohistochemistry (positive area was quantified), or
(F) by qRT-PCR
(G) qHSCs, aHSCs, and iHSCs were isolated from $Lrat^{Cre}$ (wt) and $Lrat^{\Delta PPAR\gamma}$ mice (n=8–12/group: uninjured, CCl_4-injured, or treated with rosiglitazone (5 mg/kg, daily) or vehicle for 2 weeks after CCl_4 cessation) and analyzed by qRT-PCR. * $p < 0.05$, ** $p < 0.01$, *** $p < 0.001$, student's one-way ANOVA.
(H) Primary $Lrat^{Cre}$ (wt) and $Lrat^{NF1}$-deficient qHSCs (5×10^5 cells) were treated with TGFβ1 (5 ng/ml, 24 h) ± rosiglitazone (20 μM, or vehicle), analyzed by qRT-PCR, * $p < 0.05$, ** $p < 0.01$, *** $p < 0.001$, student's one-way ANOVA.

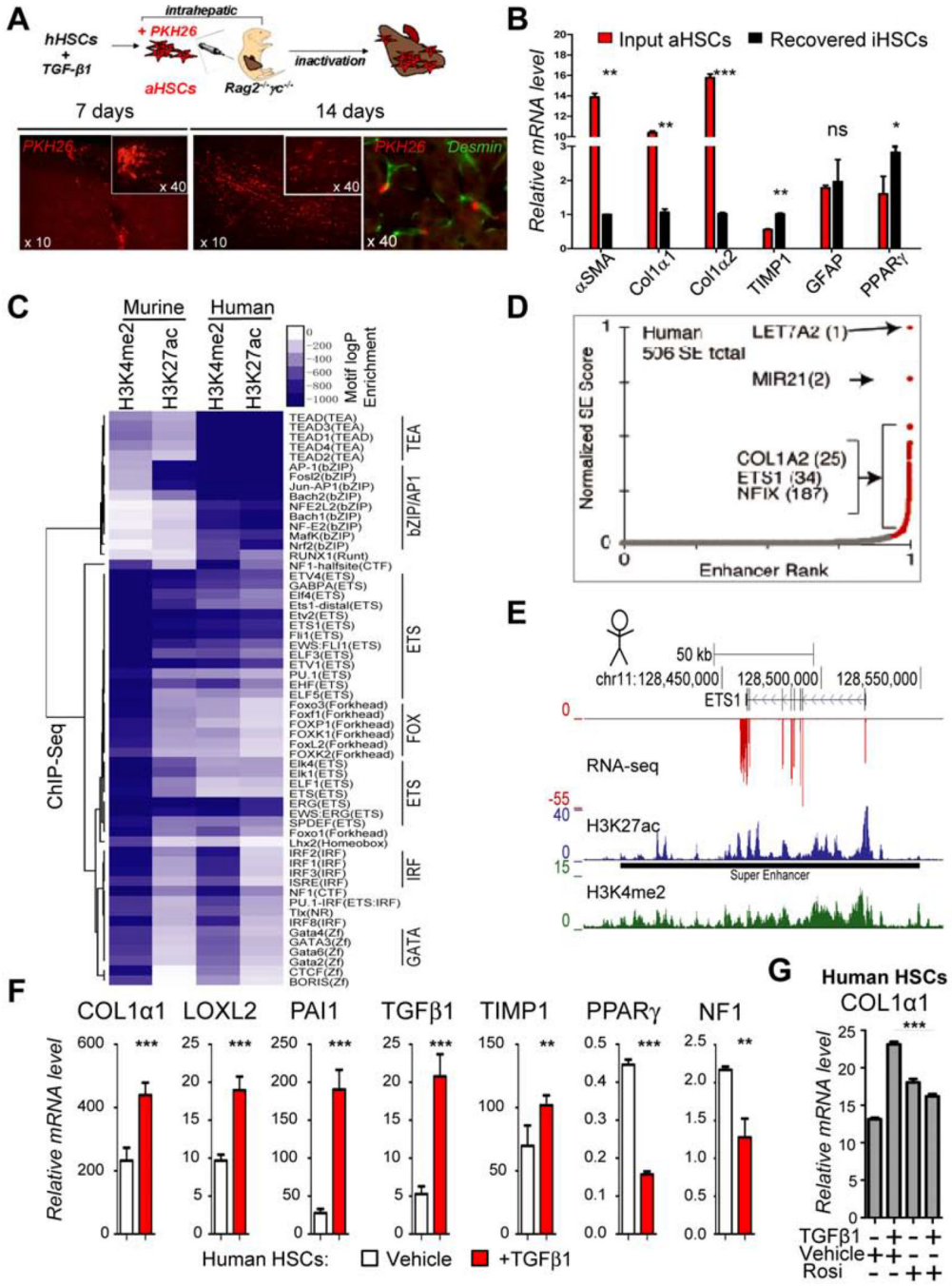

Figure 7. Identification of the lineage-determining TFs in human HSCs.

(A) PKH26-labeled TGFβ1-activated human HSCs (1×10^6 cells) were intrahepatically injected into $Rag2^{-/-}\gamma c^{-/-}$ pups (1 day old). Livers analyzed by immunohistochemistry or fluorescent microscopy (x 10 objectives or x40).

(B) Sort purified. Input and recovered human iHSCs were analyzed by qRT-PCR * $p < 0.05$, ** $p < 0.01$, *** $p < 0.001$, student's *t* test.

(C) Heatmap depicting enrichment for known transcription factor motifs in H3K27ac and H3K4me2 peaks in human and mouse HSC enhancer repertoires.

(D) Super enhancer hockey stick plot depicting the normalized level of H3K27ac signal at enhancers as a function of the enhancer rank for human HSC.
(E) Normalized RNA-seq and H3K27ac/H3K4me2 ChIP-seq read densities from primary human HSCs are depicted at the *ETS1* locus in the human genome (hg38).
(F-G) Human HSCs were treated with ± TGFβ1 (5 ng/ml, 24 h) **(F)** ± rosiglitazone (20nM, or vehicle) **(G)**, and analyzed by qRT-PCR, *$p < 0.05$, ** $p < 0.01$, *** $p < 0.001$, student's *t* test and one-way ANOVA.